Oxidation of Gas-Phase Protactinium Ions, Pa^+ and Pa^{2+}: Formation and Properties of $PaO_2^{2+}(g)$, Protactinyl

Marta Santos,[†] António Pires de Matos,*[,†] Joaquim Marçalo,[†] John K. Gibson,[‡] Richard G. Haire,[‡] Rajni Tyagi,[§] and Russell M. Pitzer[§]

Departamento de Química, Instituto Tecnológico e Nuclear, 2686-953 Sacavém, Portugal, Chemical Sciences Division, Oak Ridge National Laboratory, Box 2008, Oak Ridge, Tennessee 37831-6375, and Department of Chemistry, The Ohio State University, 100 West 18th Avenue, Columbus, Ohio 43210

Received: December 14, 2005; In Final Form: February 20, 2006

Oxidation reactions of bare and ligated, monopositive, and dipositive Pa ions in the gas phase were studied by Fourier transform ion cyclotron resonance mass spectrometry. Seven oxidants were employed, ranging from the thermodynamically robust N_2O to the relatively weak CH_2O—all oxidized Pa^+ to PaO^+ and PaO^+ to PaO_2^+. On the basis of experimental observations, it was established that $D[Pa^+-O]$ and $D[OPa^+-O] \geq 751$ kJ mol^{-1}. Estimates for $D[Pa^+-O]$, $D[OPa^+-O]$, IE[PaO], and IE[PaO_2] were also obtained. The seven oxidants reacted with Pa^{2+} to produce PaO^{2+}, indicating that $D[Pa^{2+}-O] \geq 751$ kJ mol^{-1}. A particularly notable finding was the oxidation of PaO^{2+} by N_2O to PaO_2^{2+}, a species, which formally comprises Pa(VI). Collision-induced dissociation of PaO_2^{2+} suggested the protactinyl connectivity, $\{O-Pa-O\}^{2+}$. The experimentally determined IE[PaO_2^+] $\approx$ 16.6 eV is in agreement with self-consistent-field and configuration interaction calculations for PaO_2^+ and PaO_2^{2+}. These calculations provide insights into the electronic structures of these ions and indicate the participation of 5f orbitals in bonding and a partial "6p hole" in the case of protactinyl. It was found that PaO_2^{2+} catalyzes the oxidation of CO by N_2O—such O atom transport via a dipositive metal oxide ion is distinctive. It was also observed that PaO_2^{2+} is capable of activating H_2 to form the stable PaO_2H^{2+} ion.

Introduction

Gas-phase reactions between bare and ligated metal ions have been studied extensively over the past decades to understand fundamental aspects of metal ion chemistry, as well as to provide insights into molecular and theoretical chemistries.[1] A primary focus has been on d block transition metal ions, particularly those of the ubiquitous 3d metals, notably Fe.[2] Several studies have focused on the 4f series lanthanides (Ln)[3] and the two abundant and long-lived radioactive 5f series actinides (An), thorium and uranium.[4] It has only been within the past decade that systematic studies of other, highly radioactive, actinides have been undertaken; experimental results were reported for the actinides through einsteinium.[5−8] The very versatile experimental technique of Fourier transform ion cyclotron resonance mass spectrometry (FTICR-MS) has been applied to the study of gas-phase oxidation of monopositive and dipositive ions of Np, Pu, and Am.[6−8] In the work reported here, the first FTICR-MS studies of Pa ion chemistry were carried out. The only previous study of gas-phase Pa ion chemistry employed time-of-flight mass spectrometry (TOF-MS).[9]

Protactinium is an intriguing actinide as it is the first member of the series to have a ground-state, atomic electronic configuration, $[Rn]5f^2 6d^1 7s^2$ ([Rn] represents the radon "core"), with occupation of 5f orbitals. The filling of the 5f orbitals distinguishes the actinide series. It is also the first actinide metal to exhibit bonding involving 5f electrons under STP conditions.[10] It may also have some 5f participation in bonding of some solid compounds.[11] The role of 5f electrons in the bonding of protactinium molecular complexes is generally less than in the crystalline solids but is not necessarily insignificant[12−14] and remains an issue in actinide science.

The formation and thermodynamic characterization of protactinium oxides from high-temperature vaporization of solid PaO_{2-x}[15] represent one of the few studies of protactinium molecular chemistry. The relative pressures of the three vapor species, Pa, PaO, and PaO_2, were measured, the enthalpies of formation of the species were determined, and the first, Pa−O, and second, OPa−O, bond energies were derived in that work.[15] Oxide molecules are among the most fundamental molecular species for a metal and are often the focus for advanced theoretical methods, as for example, in the case of UO_2.[16]

We report here studies of the oxidation kinetics of monopositive and dipositive bare and ligated protactinium ions and experiments to enable estimation of the ionization energy (IE) of PaO_2^+. The thermodynamics of protactinium oxides—i.e., metal-oxygen bond energies—are addressed, and the results are compared with previously reported thermodynamic values.

An additional focus of this work was to establish the existence and properties of a new species, PaO_2^{2+}, which formally comprises Pa in an unusually high-valence state, i.e., above Pa(V). These protactinium studies address an intriguing aspect of gas-phase metal ion chemistry—the possibility for the synthesis of species in which the metal is in an unusually high oxidation state, such as CeO_2^+,[17] PtO_2^+,[18] and ThO_2^+.[7,19] Theoretical calculations were performed to provide insights into the nature

* To whom correspondence should be addressed. E-mail: pmatos@itn.pt.
[†] Instituto Tecnológico e Nuclear.
[‡] Oak Ridge National Laboratory.
[§] The Ohio State University.

10.1021/jp057297d CCC: $33.50
Published on Web 04/12/2006

of this unexpected "protactinyl" species that is not found in condensed phase chemistry.[20]

Experimental Section

The experimental approach has been described in detail elsewhere.[6−8,21] The experiments were performed with a Finnigan FT/MS 2001-DT FTICR mass spectrometer, equipped with a 3T superconducting magnet and controlled by a Finnigan Venus Odyssey data system. The instrument incorporated a Spectra-Physics Quanta-Ray GCR-11 Nd:YAG laser operated at the fundamental wavelength (1064 nm) for laser desorption/ionization (LDI) of solid samples.

The starting samples were "alloys" of Pa, Th and U in a Pt matrix. The Pa sample (milligram amount of Pa-231 in Pt) was a ~5 wt % Pa product. For the electron-transfer calibration experiments, high-purity metals (>99.9%) were used. The reagent gases (N_2O, O_2, CO_2, NO, CO, H_2, N_2, and Ar) were all commercial products (>99% purity) and used as supplied. The C_2H_4O (>99% ethylene oxide) was degassed prior to its use, and the H_2O was thoroughly deoxygenated with N_2 and then degassed by multiple freeze−evacuation−thaw cycles. Dry, gaseous CH_2O was prepared according to a literature procedure.[22] These reagents were introduced into the spectrometer through leak valves to pressures in the range of 3×10^{-8} to 2×10^{-7} Torr, and their purities were confirmed from electron ionization mass spectra. The neutral reagent pressures were measured with a Bayard−Alpert type ionization gauge calibrated using standard reactions of methane[23] and acetone[24] ions, with the gauge readings being corrected for relative sensitivities.[25,26]

Metal ions were produced in the FTICR-MS by LDI of the samples so that the desorbed ions (both singly and doubly charged) directly entered the ICR source cell, where the reaction experiments were performed. Isolation of the metal ions was achieved using single-frequency, frequency sweep, or SWIFT excitation;[27] product ions formed in sufficient amounts for studying were similarly isolated. In some cases, reactant metal oxide ions were produced by reaction of metal ions with N_2O introduced into the spectrometer through a pulsed valve. All of the reactant ions were thermalized by collisions with Ar. The reproducibility of the reaction kinetics, as well as the linearity of semilog plots of normalized reactant ion intensities vs time, verified thermalization of the reactant ions. When more than one product ion formed, invariant product distributions for different collisional cooling periods and/or collision gas pressures also indicated that effective thermalization had been achieved.

Pseudo-first-order reaction rate constants, k, were determined from the decay of the reactant ion signals as a function of time, at constant neutral reagent pressures. Together with the absolute rate constants, reaction efficiencies are reported as k/k_{COL}: k_{COL} is the collisional rate constant derived from the modified variational transition-state/classical trajectory theory developed by Su and Chesnavich.[28] Collisional rate constants were calculated using experimental molecular polarizabilities and dipole moments of the neutral reagents.[26] Because of uncertainties in the pressures, uncertainties of ±50% are assigned to the reported rate constants; the relative uncertainties are estimated to be ±20%.

Results and Discussion

The O-atom affinities (OA ≡ D[R−O]) and IEs of the seven oxidants (RO) employed in this study are given in Table 1. The results for reactions of Pa^+, PaO^+, Pa^{2+}, and PaO^{2+} with these oxidants are summarized in Table 2 as reaction efficiencies, k/k_{COL}, absolute reaction rate constants, k, and product distributions. The specific reactions are discussed in individual sections below.

TABLE 1: Thermodynamics of Oxidants, RO [29]

RO	N_2O	C_2H_4O	H_2O	O_2	CO_2	NO	CH_2O
D[R−O] (kJ mol^{-1})	167	354	491	498	532	632	751
IE[RO] (eV)	12.89	10.56	12.62	12.07	13.78	9.26	10.88

Oxidation of Pa^+. As is seen from the results in Table 2, Pa^+ is efficiently oxidized to PaO^+ by each oxidant. The reaction efficiencies and the product distributions for Pa^+ are similar to those previously reported for Th^+, U^+, and Np^+ with these seven oxidants.[6,19] With N_2O, PaN^+ is also produced, indicating that D[Pa^+−N] ≥ 482 kJ mol^{-1}.[30] The relative abundance of PaN^+ (40%) is comparable to those of ThN^+ (50%), UN^+ (40%), and NpN^+ (25%) from the corresponding An^+/N_2O reactions.[6] With H_2O, $PaOH^+$ formed (30%) in addition to PaO^+; for comparison, the Th^+/H_2O reaction produced $ThOH^+$ (35%), but hyperthermal conditions were required to produce UOH^+ and $NpOH^+$.[6] Jackson et al.[31] observed a 10% UOH^+ product channel for the U^+/H_2O reaction in a quadrupole ion trap, possibly indicating the presence of slightly kinetically excited U^+ ions. If $PaOH^+$ is indeed a hydroxide, it could be concluded that D[Pa^+−OH] ≥ 499 kJ mol^{-1}.[30] However, a recent matrix isolation study of UO_xH_y molecules casts doubt on the assumption about a hydroxide structure.[32] Specifically, it was shown that the most stable structure of the neutral species with composition UO_2H_2 is the U(VI) oxyhydride, H_2UO_2, and not a hydroxide.[32] Thus, $PaOH^+$ may correspond to the oxyhydride, {H−Pa═O}$^+$, which would be comprised of stable Pa(IV).

With the reagents N_2O, H_2O, CO_2, NO, and CH_2O, the ions Th^+, Pa^+, U^+, and Np^+ are significantly more reactive than Pu^+ and Am^+.[6,7] The reactivity of an An^+ ion toward a particular oxidant can of course reflect kinetics rather than thermodynamics[6,7]—exothermicity is a necessary but not sufficient condition for a reaction to occur. The first six An^+ ions (Th^+ through Am^+) are oxidized to AnO^+ by C_2H_4O, indicating that D[An^+−O] is at least 354 kJ mol^{-1}, so that their oxidation by N_2O should be exothermic by at least 187 kJ mol^{-1}. Whereas Th^+, U^+, and Np^+ are efficiently oxidized by N_2O ($k/k_{COL} \geq 0.5$), Pu^+ and Am^+ are inefficiently oxidized by it ($k/k_{COL} = 0.02$ and 0.004, for Pu^+ and Am^+, respectively[6,7]). There is an indication that a kinetic barrier exists for some An^+/N_2O reactions, and an inverse correlation is found between An^+ reactivity and the promotion energy from the ground electronic state to a "divalent" reactive configuration with at least two spin-unpaired non-5f valence electrons. Thus, the higher the promotion energy is, the lower the reactivity of the ion is.[6,7] In the ground-state configuration of Pa^+, $5f^2 7s^2$,[33] the $7s^2$ valence electrons are spin-paired so that the lowest-lying "divalent" reactive configuration is $5f^2 6d7s$, which lies only 0.10 eV higher in energy.[33] In view of this small promotion energy, the observed high reactivity of Pa^+ toward N_2O should be expected. It is possible that the 5f electrons of Pa^+ may also participate directly in bond activation.

Oxidation of Pa^+ by CH_2O indicates that D[Pa^+−O] ≥ 751 kJ mol^{-1}. Kleinschmidt and Ward[15] have reported D[Pa−O] = 788 ± 17 kJ mol^{-1}. For other actinides (Th, U, Np, Pu, and Am), it has been shown that the IE[An] and the IE[AnO] are within ~0.3 eV of one another.[7,34−36] If it is assumed that IE[PaO] ≈ IE[Pa] = 5.89 ± 0.12 eV,[37] then D[Pa^+−O] ≈ D[Pa−O] = 788 kJ mol^{-1} is derived using eq 1 (1 eV = 96.4853 kJ mol^{-1}).

$$D[M^+-O] = D[M-O] + IE[M] - IE[MO] \qquad (1)$$

TABLE 2: Results for Reactions of Pa^+, PaO^+, Pa^{2+}, and PaO^{2+} with Oxidants[a]

	N_2O	C_2H_4O	H_2O	O_2	CO_2	NO	CH_2O
Pa^+	0.49 (3.4) PaO^+/60% PaN^+/40%	0.44 (7.5) PaO^+/100%	0.26 (5.7) PaO^+/70% $PaOH^+$/30%	0.66 (3.6) PaO^+/100%	0.38 (2.5) PaO^+/100%	0.51 (3.2) PaO^+/100%	0.48 (10.6) PaO^+/100%
PaO^+	0.48 (3.4) PaO_2^+/100%	0.43 (7.4) PaO_2^+/100%	0.19 (4.3) PaO_2H^+/60% PaO_2^+/40%	0.65 (3.6) PaO_2^+/100%	0.41 (2.7) PaO_2^+/100%	0.33 (2.1) PaO_2^+/100%	0.39 (8.5) PaO_2^+/100%
Pa^{2+}	0.40 (5.6) PaO^{2+}/60% PaN^+/40%	0.31 (10.6) PaO^+/75% PaO^{2+}/25%	0.18 (7.9) $PaOH^{2+}$/100%	0.55 (6.1) PaO^{2+}/100%	0.38 (5.0) PaO^{2+}/100%	0.34 (4.2) Pa^+/75% PaO^{2+}/25%	0.17 (7.4) PaO^{2+}/90% PaO^+/10%
PaO^{2+}	0.34 (4.8) PaO_2^{2+}/100%	0.30 (10.2) PaO_2^+/100%	NS[b]	<0.001 (<0.01)	<0.001 (<0.01)	ND[b] PaO^+/100%	0.15 (6.6) $PaOH^+$/100%

[a] The reaction efficiencies, k/k_{COL}, are given; the values in brackets are the pseudo-first-order reaction rate constants, k, in units of 10^{-10} cm^3 molecule^{-1} s^{-1}. The absolute values are considered accurate to ±50%; the relative values for comparative purposes are considered accurate to ±20%. [b] NS, not studied; ND, not determined.

In the absence of an experimental value for IE[PaO], we estimate that $D[Pa^+-O] = 800 \pm 50$ kJ mol^{-1}—this value is based on the assigned lower limit of 751 kJ mol^{-1} and the assumption that IE[PaO] = IE[Pa] ± 0.5 eV. Our estimate of $D[Pa^+-O] \approx 800$ kJ mol^{-1} is close to values reported for $D[U^+-O]$.[6] This estimate for $D[Pa^+-O]$ is also in accord with systematic trends across the actinide series[6,7] and was estimated from a TOF-MS study of gas-phase Pa^+ chemistry.[9] Furthermore, a semiempirical model of bonding in actinide oxides has arrived at the same estimate.[38] Using $\Delta H_f[Pa^+] = 1138 \pm 33$ kJ mol^{-1} [39] and $\Delta H_f[O] = 249$ kJ mol^{-1},[30] the $D[Pa^+-O] = 800 \pm 50$ kJ mol^{-1} value gives $\Delta H_f[PaO^+] = 587 \pm 60$ kJ mol^{-1}. Alternatively, using $\Delta H_f[PaO] = 10 \pm 17$ kJ mol^{-1} from Kleinschmidt and Ward[15] and IE[PaO] = 5.9 ± 0.5 eV, we obtain a slightly lower value of $\Delta H_f[PaO^+] = 579 \pm 51$ kJ mol^{-1}.

Oxidation of PaO^+. The PaO^+ ion was oxidized to PaO_2^+ by each of the oxidants, as indicated in Table 2, and its efficient oxidation by CH_2O indicates that $D[OPa^+-O] \geq 751$ kJ mol^{-1}. In contrast, other AnO^+ (An = Th, U, Np, Pu, and Am) are not oxidized by CH_2O under thermal conditions.[6,7] For the other AnO^+/NO reactions that have been studied (An = Th, U, Np, Pu, and Am),[6,7] only UO^+ was oxidized, with an efficiency of $k/k_{COL} = 0.11$. As discussed,[7] it appears that oxidation of heavy metal ions by NO is kinetically favorable and that oxidation rates correlate with reaction exothermicities. On the basis of the nonoxidation of UO^+ by CH_2O and the oxidation efficiency of PaO^+ by NO, we conclude that $D[OPa^+-O] > D[OU^+-O]$. This relationship was also inferred from the greater yield of PaO_2^+ vs UO_2^+ during laser ablation of solid oxides.[9]

The IE of a metal dioxide is related to the bond energies and monoxide IE according to eq 2.

$$IE[MO_2] = D[OM-O] - D[OM^+-O] + IE[MO] \quad (2)$$

Using eq 2 and $D[OPa-O] = 772 \pm 17$ kJ mol^{-1} from Kleinschmidt and Ward,[15] $D[OPa^+-O] \geq 751$ kJ mol^{-1} from the present results, and IE[PaO] = 5.9 ± 0.5 eV that was estimated above, we obtain $IE[PaO_2] \leq 6.1 \pm 0.6$ eV. Considering the above inference that $D[OPa^+-O] > D[OU^+-O]$ and the literature values $D[OU^+-O] = 764 \pm 24$ kJ mol^{-1} [30] and $D[OU^+-O] = 772 \pm 56$ kJ mol^{-1},[39] we can tentatively estimate $D[OPa^+-O] \approx D[OPa-O]$; therefore, $IE[PaO_2] \approx IE[PaO] = 5.9 \pm 0.5$ eV. From systematic trends in IEs for AnO and AnO_2 where an oxidation state greater than An(IV) is accessible[36] {e.g., IE[UO] = 6.03 eV and $IE[UO_2] = 6.13$ eV;[35] IE[NpO] = 6.1 eV and $IE[NpO_2] = 6.33$ eV;[36] IE[PuO] = 6.1 eV and $IE[PuO_2] = 7.02$ eV;[6,7,36] and IE[AmO] = 6.2 eV and $IE[AmO_2] = 7.23$ eV[7,36]}, our estimate that $IE[PaO_2] \approx IE[PaO]$ may reflect the stability of Pa(V) and a decreasing stability of An(V) when progressing from U to Am. Using $IE[PaO_2] = 5.9 \pm 0.5$ eV, together with $\Delta H_f[PaO_2] = -513 \pm 17$ kJ mol^{-1},[15] yields $\Delta H_f[PaO_2^+] = 56 \pm 51$ kJ mol^{-1}.

Reactions of PaN^+ and $PaOH^+$. The PaN^+ product formed in the Pa^+/N_2O reaction (see Table 2) was found to react with a second N_2O molecule to produce $PaNO^+$; its structure is not known. This oxidation reaction proceeds with a rate constant $k = 2.2 \times 10^{-10}$ cm^3 molecule^{-1} s^{-1} ($k/k_{COL} = 0.32$). For comparison, the reactions of ThN^+ and UN^+ with N_2O were also examined. The ThN^+/N_2O rate constant is $k = 0.43 \times 10^{-10}$ cm^3 molecule^{-1} s^{-1} ($k/k_{COL} = 0.06$) with the product distribution being 80% ThO^+ and 20% $ThNO^+$; UN^+ was unreactive with N_2O within our detection limit (i.e., $k < 0.01 \times 10^{-10}$ cm^3 molecule^{-1} s^{-1}; $k/k_{COL} < 0.001$); this in accord with a previous report.[40]

The reactivity of PaN^+ with N_2O is very different from those of ThN^+ and UN^+. It has been shown[40] that the oxidation of UN^+ by N_2O is highly exothermic and must be kinetically hindered. Although UO^{2+} and UN^+ are isoelectronic, UO^{2+} is readily oxidized to UO_2^{2+} by N_2O.[8,41] The greater reactivity of UO^{2+} as compared with UN^+ might be attributed to the greater electrophilicity of dipositive ions[1d] (presumably $IE[UO^+] > IE[UN]$). In a SIFT-MS study of the oxidation of 46 monopositive metal ions by N_2O by Lavrov et al.,[42] only six—Ti^+, Zr^+, Nb^+, Ta^+, Os^+, and La^+—formed MN^+ as a primary product, and only three of these—NbN^+, TaN^+, and OsN^+—formed MNO^+ as a secondary product.

Heinemann and Schwarz[40] and Zhou and Andrews[43] have both shown that the structure of UNO^+ is $\{N-U-O\}^+$, which is isoelectronic with UO_2^{2+}. Neutral ThNO was produced by insertion of Th into NO (structure, {N−Th−O}), with the bonding characterized as being comparable to that in OThO but with one less nonbonding electron.[43] A probable structure for $PaNO^+$ is $\{N-Pa-O\}^+$, which is isoelectronic with PaO_2^{2+} discussed below.

The primary product of the Pa^+/H_2O reaction, $PaOH^+$ (see Table 2), reacted with a second H_2O molecule to produce PaO_2^+ (85%) and PaO_2H^+ (15%), with an overall rate constant of $k = 3.4 \times 10^{-10}$ cm^3 molecule^{-1} s^{-1} ($k/k_{COL} = 0.16$). The PaO_2H^+ ion is probably an oxide hydroxide, $\{O=Pa-OH\}^+$, where the metal center is tetravalent.

Oxidation of Pa^{2+}. The reactions of Pa^{2+} with the oxidants studied are included in Table 2. In each case, the reaction efficiency was high—at least 17%. The PaO^{2+} product was dominant with all oxidants except with (a) H_2O where $PaOH^{2+}$ was the sole product, (b) C_2H_4O where PaO^+ was the favored product together with 25% PaO^{2+}, and (c) NO where Pa^+ was the main product together with 25% PaO^{2+}. Electron transfer

in the case of NO is in accord with this reagent having an IE ca. 2.4 eV (see Table 1) below IE[Pa^+] = 11.7 ± 0.5 eV.[39] The product distributions and reaction efficiencies for Pa^{2+} are similar to those previously reported for Th^{2+} and U^{2+} with the same oxidants.[8,41] The exceptions to this similarity were H_2O, where Th^{2+} also formed 10% ThO^{2+}, and CH_2O, where U^{2+} did not form UO^{2+} but yielded UH^+ as the major product (80%).[8]

Because Pa^{2+} was oxidized to PaO^{2+} by CH_2O, it is concluded that D[Pa^{2+}−O] ≥ 751 kJ mol^{-1}. In the study of oxidation of other An^{2+} ions (An = Th, U, Np, Pu, and Am),[8] under thermoneutral conditions, only Th^{2+} is oxidized to ThO^{2+} by CH_2O. It is reasonable to infer that the Th^{2+}−O and Pa^{2+}−O bonds are stronger than are the An^{2+}−O bonds for these other actinides. The stability of Th(IV) is well-known[44] and consistent with the exceptionally strong Th^{2+}−O bond. Our results indicate a greater stability of Pa(IV) as compared with An(IV) for higher members of the series.

The oxidation of Pa^{2+} by CH_2O can be used to establish an upper limit to the formation enthalpy of PaO^{2+} through the relationship, $\Delta H_f[PaO^{2+}] \leq \{\Delta H_f[Pa^{2+}] - D[CH_2-O] + \Delta H_f[O]\}$. Using $\Delta H_f[Pa^{2+}] = 2268 \pm 59$ kJ mol^{-1},[39] D[CH_2−O] = 751 kJ mol^{-1} (Table 1), and $\Delta H_f[O] = 249$ kJ mol^{-1},[30] we obtain $\Delta H_f[PaO^{2+}] \leq 1766 \pm 59$ kJ mol^{-1}. An upper limit for the second IE of PaO, IE[PaO^+] = $\{\Delta H_f[PaO^{2+}] - \Delta H_f[PaO^+]\} \leq 12.2 \pm 0.9$ eV, can be obtained from the upper limit for $\Delta H_f[PaO^{2+}]$ calculated above and $\Delta H_f[PaO^+] = 587 \pm 60$ kJ mol^{-1} estimated in a previous section. This average limit for IE[PaO^+] corresponds to an effective limit of 13.1 eV, which can be compared with equivalent limits estimated for the cases of Th (IE[ThO^+] ≤ 12.8 eV) and U (IE[UO^+] ≤ 13.8 eV) in previous work.[8]

The $PaOH^{2+}$ ion formed in the Pa^{2+}/H_2O reaction transferred a proton to a water molecule, forming PaO^+ with a rate constant $k = 16.8 \times 10^{-10}$ cm^3 molecule^{-1} s^{-1} and an efficiency $k/k_{COL} = 0.38$. This behavior of $PaOH^{2+}$ is similar to that found previously for UOH^{2+} and $NpOH^{2+}$, which similarly reacted with efficiencies, k/k_{COL}, of 0.34 and 0.27, respectively.[8]

Oxidation of PaO^{2+}—Formation of "Protactinyl": PaO_2^{2+}. The reactions of PaO^{2+} with the oxidants studied are summarized in Table 2; its reaction with H_2O was not studied. PaO^{2+} was unreactive with O_2 and CO_2; the absence of electron transfer from O_2 (IE = 12.07 eV, Table 1) is in agreement with IE[PaO^+] ≤ 13.1 eV established in the previous section, since a minimum exothermicity of ca. 1 eV is necessary for electron transfer from a neutral molecule to a dipositive ion to occur.[45,46] With NO, the oxidant with the lowest IE (see Table 1), electron transfer was the only reaction channel observed. With C_2H_4O and CH_2O, the charge-separation products were PaO_2^+ (+ $C_2H_4^+$) and $PaOH^+$ (+ HCO^+), respectively. In our previous study of the reactivity of AnO^{2+} ions with oxidants,[8] ThO^{2+} and UO^{2+} were also found to react with NO exclusively via electron transfer. With C_2H_4O, ThO^{2+} formed $ThOH^+$ (40%) and ThO_2H^+ (60%), while UO^{2+} produced UOH^+ (40%) and UO_2^+ (60%), with reaction efficiencies k/k_{COL} of 0.22 and 0.21, respectively;[8] the sole formation of PaO_2^+ with C_2H_4O (k/k_{COL} = 0.30) may reflect the exceptional stability of this formally Pa(V) ion. Similar to the case with PaO^{2+}, ThO^{2+} formed only the $ThOH^+$ ion in the reaction with CH_2O, with a comparable efficiency ($k/k_{COL} = 0.13$).[8]

Notably, N_2O was found to react with PaO^{2+} to yield PaO_2^{2+} exclusively, according to eq 3.

$$PaO^{2+} + N_2O \rightarrow PaO_2^{2+} + N_2 \quad (3)$$

It is remarkable that PaO_2^{2+} is produced and that the reaction proceeds with such a high efficiency ($k/k_{COL} = 0.34$). The oxidation of PaO^{2+} by N_2O indicates that D[OPa^{2+}−O] ≥ 167 kJ mol^{-1}. As noted above, other gas-phase species with metal ions in unusually high oxidation states, such as ThO_2^+,[6,19] have also been produced by gas-phase oxidation reactions. An unusual aspect of PaO_2^{2+} is that it is a doubly charged ion in which the metal center is in the unusually high formal oxidation state, Pa(VI). This "protactinyl"[47] product, PaO_2^{2+}, where Pa is formally in a hexavalent oxidation state, is unknown in condensed-phase chemistry.[20] Other actinyls, UO_2^{2+}, NpO_2^{2+}, PuO_2^{2+}, and AmO_2^{2+}, are well-known in condensed-phase actinide chemistry,[44] reflecting the accessibility of the An(VI) oxidation state for the four actinides following Pa.[20]

A mass spectrum illustrating the formation of PaO_2^{2+} from the reaction of Pa^{2+} with N_2O is shown in Figure 1. As shown in eq 3, the sole product of the PaO^{2+}/N_2O reaction is PaO_2^{2+}. The PaN^+ peak in Figure 1 is from the Pa^{2+}/N_2O reaction, and the $PaNO^+$ peak is from the PaN^+/N_2O reaction. The PaO_2^+ peak in Figure 1 is due to electron transfer from N_2O to PaO_2^{2+} (see below).

Three plausible structures for PaO_2^{2+} are shown in Scheme 1. Subjecting PaO_2^{2+} to collision-induced dissociation (CID) resulted in loss of a single O-atom; elimination of two O-atoms was not observed. Increasing the CID excitation energy resulted in loss of ion signal without additional fragmentation products. Similar CID experiments with linear UO_2^{2+} and NpO_2^{2+} gave the same result, exclusive loss of an O-atom. The CID results for PaO_2^{2+} are thus consistent with a $\{O-Pa-O\}^{2+}$ actinyl type of atomic connectivity: structure 1 in Scheme 1. In a theoretical study, Straka et al.[14] reported that PaO_2^+, like isoelectronic UO_2^{2+}, is linear, whereas isoelectronic ThO_2 has a bent structure. The structures of PaO_2^{2+} and isoelectronic ThO_2^+ were not described in that work.

Oxidation of CO by N_2O Mediated by PaO_2^{2+}. The reaction of PaO_2^{2+} with CO was studied by isolating Pa^{2+}, pulsed injecting N_2O to produce PaO_2^{2+}, and then allowing the isolated PaO_2^{2+} ions to react with CO present at constant pressure. It was found that PaO_2^{2+} reacts with CO to produce PaO^{2+} (+ CO_2; 50% branching ratio) and PaO_2^+ (+ CO^+; 50% branching ratio) as shown in eqs 4 and 5.

$$PaO_2^{2+} + CO \rightarrow PaO^{2+} + CO_2 \quad (4)$$

$$PaO_2^{2+} + CO \rightarrow PaO_2^{+} + CO^{+} \quad (5)$$

The overall rate constant for the PaO_2^{2+}/CO reaction is $k = 6.5 \times 10^{-10}$ cm^3 molecule^{-1} s^{-1} and the overall efficiency $k/k_{COL} = 0.22$. Combining eqs 3 and 4 indicates that PaO^{2+} should catalyze the oxidation of CO by N_2O according to the net reaction given by eq 6.

$$N_2O + CO \rightarrow N_2 + CO_2 \quad (6)$$

To demonstrate this catalytic O-atom transfer process, Pa^{2+} was exposed to a mixture of N_2O and CO. The Pa^{2+} was oxidized by N_2O, and the PaO_2^{2+} product was isolated at $t = 0$ in Figure 2. The subsequent ingrowth of PaO^{2+} in Figure 2 reflects the oxidation of CO according to eq 4. The dominant PaO_2^+ product is due to the electron-transfer reactions given by eqs 5 and 7. This catalytic effect is also evident in the kinetic plot given in Figure 3, which corresponds to the data shown in

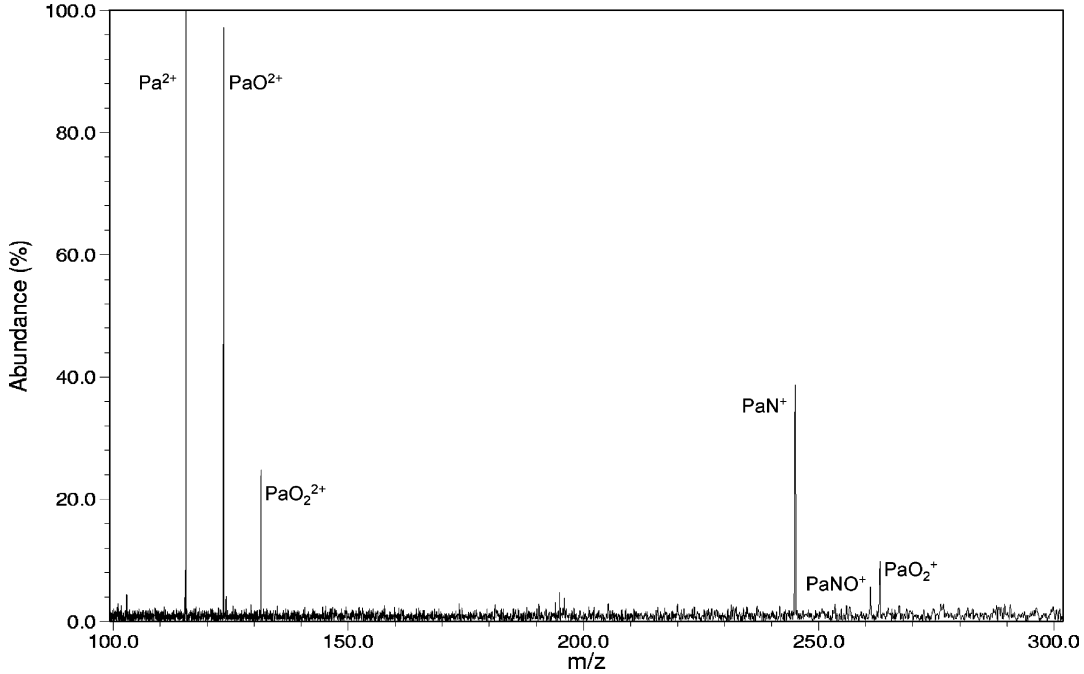

Figure 1. Mass spectrum for the Pa^{2+}/N_2O reaction, showing evidence for PaO_2^{2+}, protactinyl. The conditions were as follows: 9.8×10^{-8} Torr N_2O, ca. 1×10^{-6} Torr Ar, and a reaction time of 0.4 s.

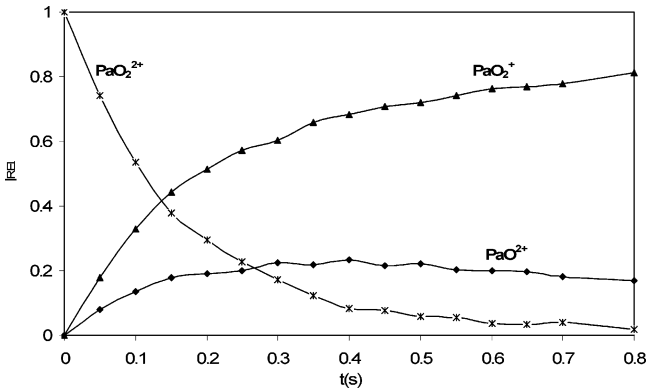

Figure 2. Plot showing the temporal evolution of the reactant ion, PaO_2^{2+}, and the product ions, PaO^{2+} and PaO_2^{+}, in an N_2O/CO mixture. The conditions were as follows: 4.8×10^{-8} Torr N_2O, 9.8×10^{-8} Torr CO, and a reaction period of 0.3 s prior to the isolation of PaO_2^{2+} at $t = 0$.

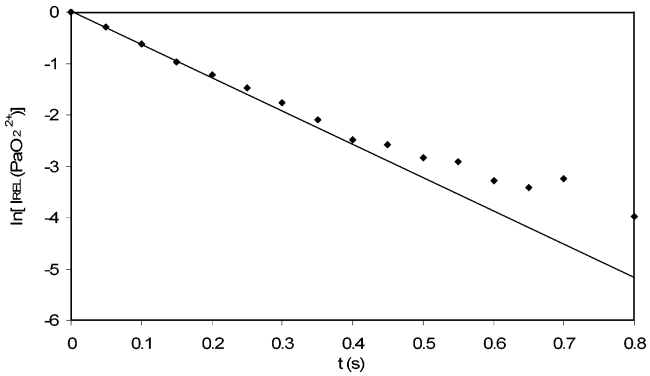

Figure 3. Kinetic plot for the reactant ion, PaO_2^{2+}. The conditions were the same as those for Figure 2.

SCHEME 1

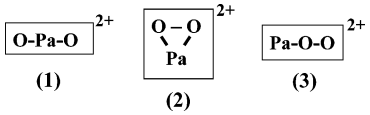

(1) (2) (3)

Figure 2—the quantity $\ln[I_{REL}(PaO_2^{2+})]$ on the *y*-axis in Figure 3 is $\ln[I(PaO_2^{2+})/\{I(PaO_2^{2+}) + I(PaO_2^{+}) + I(PaO^{2+})\}]$ [$I(PaO_n^{x+})$ is the ion intensity]. In Figure 3, the depletion of PaO_2^{2+} according to pseudo-first-order kinetics for the first ~0.4 s after isolation—i.e., the linear segment of data points—is attributed to the reactions given by eqs 4, 5, and 7. The catalytic cycle represented by eq 6 is revealed by the positive deviation from pseudo-first-order kinetics for $t > 0.4$ s, where regeneration of PaO_2^{2+} from PaO^{2+} via eq 3 is apparent.

The thermodynamic requirement for transfer of an O-atom from N_2O to CO via PaO_2^{2+} is that the oxygen affinity of PaO^{2+} lies between those of N_2 and CO: $D[N_2-O]$ (167 kJ mol^{-1}) $\leq$ $D[OPa^{2+}-O] \leq D[CO-O]$ (532 kJ mol^{-1}). Kappes and Staley[48] first demonstrated metal ion-catalyzed gas-phase oxidation of CO by N_2O employing the Fe^{+}/FeO^{+} couple for O-atom transport. Several examples of this type of gas-phase metal ion-mediated catalytic oxidation have been reported.[49] The oxidation of CO by N_2O, catalyzed by polyatomic metal oxide ions, MO_n^{+} ($n > 1$), has also been reported[49] including, notably, O-transport from N_2O to CO via PtO_2^{+}.[18]

To the best of our knowledge, the present results for PaO_2^{2+} represent the first reported example of O-atom transport between neutral molecules via a dipositive metal oxide ion. Because the second IEs of metal oxide ions are substantially greater than their first IEs and are also greater than the first IEs of many neutrals, electron abstraction becomes a significant process for dipositive metal oxides. Both eqs 5 and 7 occur in the case of PaO_2^{2+}.

$$PaO_2^{2+} + N_2O \rightarrow PaO_2^{+} + N_2O^{+} \qquad (7)$$

The rate constant for eq 7 is 7.4×10^{-10} cm^3 molecule^{-1} s^{-1}, and the efficiency is $k/k_{COL} = 0.53$. By converting PaO_2^{2+} to monopositive PaO_2^{+}, which according to thermodynamic consideration will not transfer an O-atom to CO since $D[OPa^{+}-O] \geq 751$ kJ mol^{-1} and $D[CO-O] = 532$ kJ mol^{-1} (Table 1), the electron-transfer reactions given by eqs 5 and 7 terminate the catalytic cycle. The catalytic cycle is summarized in

SCHEME 2

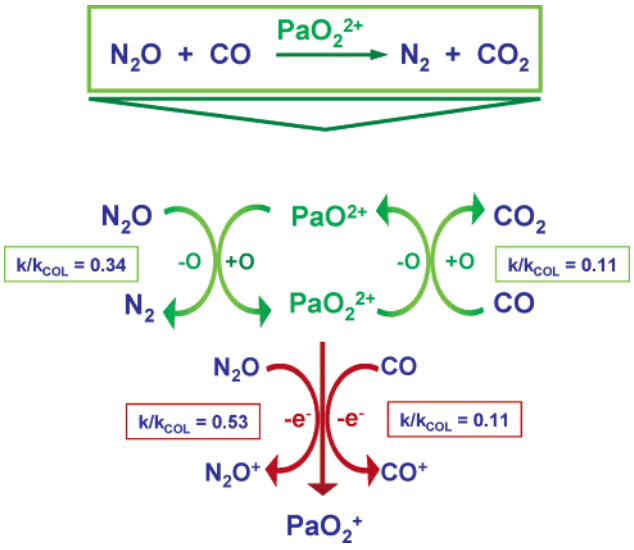

Scheme 2, where the O-transfer processes (eqs 3 and 4) represent the PaO^{2+}-catalyzed oxidation of CO by N_2O and the electron-transfer processes (eqs 5 and 7) represent the termination of the cycle by elimination of PaO_2^{2+}. In the absence of the electron-transfer reactions (eqs 5 and 7), the concentrations of PaO_2^{2+} and PaO^{2+} would hypothetically approach equilibrium values. This is not seen in Figures 2 and 3 because of the depletion of PaO_2^{2+} by electron transfer, i.e., the ingrowth of PaO_2^{+} shown in Figure 2.

As a result of the relatively high efficiencies of the electron-transfer reactions (eqs 5 and 7), the overall turnover rate for the catalytic cycle shown in Scheme 2 must be low. The rate constant for eq 5 is 3.2×10^{-10} cm^3 molecule^{-1} s^{-1}, whereas the sum of the rate constants for eqs 5 and 7 is 10.6×10^{-10} cm^3 molecule^{-1} s^{-1}. Under equal pressures of N_2O and CO, it is about three times more likely that the cycle will be terminated than it is to have oxidation of CO by PaO_2^{2+}; under all conditions, the net turnover rate will be less than one CO oxidation per PaO_2^{2+}.

Activation of H_2 by PaO_2^{2+}. In view of the ability of PaO_2^{2+} to mediate the oxidation of CO by N_2O, two other prototypical substrates, H_2 and CH_4, were examined under identical conditions used for the CO/N_2O studies. Because of the relatively low IE of CH_4 (IE[CH_4] = 12.51 eV[30]), the only reaction of PaO_2^{2+} observed in a CH_4/N_2O mixture was electron transfer to yield PaO_2^{+}. Conversely, PaO_2^{2+} activated molecular hydrogen (IE[H_2] = 15.43 eV[30]) to produce exclusively PaO_2H^{2+}, with a rate constant $k = 4.3 \times 10^{-10}$ cm^3 molecule^{-1} s^{-1} and an efficiency $k/k_{COL} = 0.14$. The PaO_2H^{2+} ion is presumably the pentavalent oxide hydroxide, $\{O{=}Pa^{V}{-}OH\}^{2+}$ as seen in aqueous solutions,[20] and it should be a stable species. The formation of PaO_2H^{2+} from the PaO_2^{2+}/H_2 reaction indicates that D[PaO_2^{2+}−H] ≥ D[H−H] = 436 kJ mol^{-1}.[30] The PaO_2H^{2+} ion reacted with N_2O from the neutral reagent mixture by proton transfer to give PaO_2^{+} (+ [H,N_2O]$^{+}$), with a rate constant $k = 5.0 \times 10^{-10}$ cm^3 molecule^{-1} s^{-1} and an efficiency $k/k_{COL} = 0.34$.

Electron Transfer to PaO_2^{2+}—The IE of PaO_2^{+}. The relative efficiencies of electron transfer from N_2O (IE = 12.89 eV) to UO_2^{2+} ($k/k_{COL} = 0.02$), NpO_2^{2+} ($k/k_{COL} = 0.49$), and PuO_2^{2+} ($k/k_{COL} = 0.42$) were previously measured to estimate the second IEs of the three AnO_2^{2+},[8] and details of application of the charge-transfer method to actinyl ions have been described there. None of those three AnO_2^{2+} abstracted an electron from CO_2 (IE = 13.78 eV), while in contrast, PaO_2^{2+} abstracted an electron from CO_2 with an efficiency of 0.51. It is apparent that IE[PaO_2^{+}] is significantly larger than IE[UO_2^{+}] = 14.6 ± 0.4 eV, IE[NpO_2^{+}] = 15.1 ± 0.4 eV, and IE[PuO_2^{+}] = 15.1 ± 0.4 eV, and it was necessary to employ an electron-transfer reagent with an IE greater than that of CO_2 to estimate the IE of PaO_2^{+}.

As discussed above, PaO_2^{2+} abstracts an electron from CO (IE = 14.01 eV), as an alternative reaction pathway to O-atom transfer (see Scheme 2). The relative efficiency for electron transfer from CO is 0.11. Because this electron-transfer reaction competes with O-atom transfer, its intrinsic efficiency should be slightly greater than 0.11. As discussed by Roth and Freiser,[45] the efficiency of electron transfer from a neutral molecule to a dipositive ion exhibits a distinct positive correlation with the exothermicity of the process—the more exothermic an electron-transfer reaction is, the more efficiently it will proceed. For electron transfer from a neutral molecule to a dipositive ion to occur, some miminum exothermicity, typically ~1 eV, is required.[45,46] Roth and Freiser[45] also indicated that the efficiency of such electron-transfer processes is generally independent of the nature of the dipositive ion.[50] Accordingly, it is valid to employ a calibration of efficiency vs exothermicity using doubly charged bare metal ions to estimate IEs of oxo-ligated MO_2^{2+}, as done and discussed previously for other AnO_2^{2+}.[8]

To estimate IE[PaO_2^{+}] from the electron-transfer efficiency with CO, such a calibration approach was performed. The quantity $\Delta E[M^{2+}/X]$ is defined as the exothermicity associated with electron transfer from the neutral reagent X to the dipositive M^{2+} ion: $\Delta E[M^{2+}/X] = IE[X] - IE[M^{+}]$. As $\Delta E[Sn^{2+}/CO] = 0.62$ eV[26] is well below the ~1 eV threshold for the onset of electron transfer from a neutral to a dipositive ion,[59,60] the measured electron-transfer efficiencies with CO were adjusted downward using the very small measured $k/k_{COL} = 0.005$ for the Sn^{2+}/CO electron-transfer reaction. The minor degree of electron transfer from nominally pure CO to Sn^{2+} is attributed to a small amount of air (and possibly other impurities) introduced with the CO reagent gas. In particular, $\Delta E[Sn^{2+}/O_2] = 2.56$ eV, so that electron transfer from an O_2 impurity to Sn^{2+} should be quite efficient (similar to that for Bi^{2+}/CO): <1% O_2 in the CO could account for the apparent but implausible electron transfer from "CO" to Sn^{2+}. Also, $\Delta E[Sn^{2+}/H_2O] = 2.01$ eV indicates that small amounts of water in the CO could also contribute to the minor electron-transfer reaction to Sn^{2+}. The extent of electron transfer from impurities should be essentially the same for the other dications, so that the reported k/k_{COL} values were reduced by 0.005 determined from the reaction of Sn^{2+} with "CO". This small adjustment does not affect the overall interpretation of the results. The following (background-corrected) electron-transfer efficiencies were determined, with the corresponding $\Delta E[M^{2+}/CO]$ indicated in brackets:[26] $k/k_{COL} = 0.002$ for Pb^{2+} {$\Delta E[Pb^{2+}/CO] = 1.02$ eV}; $k/k_{COL} = 0.017$ for Mn^{2+} {$\Delta E[Mn^{2+}/CO] = 1.63$ eV}; $k/k_{COL} = 0.027$ for Ge^{2+} {$\Delta E[Ge^{2+}/CO] = 1.92$ eV}; $k/k_{COL} = 0.24$ for Bi^{2+} {$\Delta E[Bi^{2+}/CO] = 2.68$ eV}. The very inefficient electron transfer for Pb^{2+}/CO is consistent with an onset threshold of $\Delta E[M^{2+}/X] \approx 1$ eV.[45,46]

The electron-transfer efficiency for PaO_2^{2+} (placed at 0.11; may be slightly greater due to the competing O-transfer channel) is at least three times that for Ge^{2+} (0.027) and approximately half of that for Bi^{2+} (0.24). Accordingly, we conclude that IE[Ge^{+}] < IE[PaO_2^{+}] < IE[Bi^{+}] and that IE[PaO_2^{+}] is slightly smaller than IE[Bi^{+}] = 16.69 eV. Thus, the resulting estimate is IE[PaO_2^{+}] = 16.6 ± 0.4 eV.

As described above, PaO_2^{2+} reacted with H_2 (IE[H_2] = 15.43 eV[30]) to form the PaO_2H^{2+} ion (with $k/k_{COL} = 0.14$). Given the efficient H-atom transfer from H_2, it is possible that a minor (i.e., $k/k_{COL} < 0.01$) electron-transfer channel may not have been detected. PaO_2^{2+} did not react with N_2 (IE[N_2] = 15.58 eV[30]) or Ar (IE[Ar] = 15.76 eV[30]), consistent with IE[PaO_2^+] = 16.6 ±0.4 eV and a minimum ΔE of ~1 eV that is needed for electron transfer.

Thermodynamics and Stability of PaO_2^{2+}. The enthalpy of formation of a MO_2^{2+} species in the gas phase can be evaluated from the relationship given in eq 8.

$$\Delta H_f[MO_2^{2+}(g)] = \Delta H_f[MO_2(g)] + IE[MO_2] + IE[MO_2^+] \quad (8)$$

Before applying eq 8 to PaO_2^{2+}, its validity was assessed for UO_2^{2+} and PuO_2^{2+}. The following values are employed on the right-hand side of eq 8: $\Delta H_f[UO_2(g)] = -467$ kJ mol^{-1};[51] $\Delta H_f[PuO_2(g)] = -422$ kJ mol^{-1};[51] IE[UO_2] = 6.13 eV;[36] IE[PuO_2] = 7.02 ± 0.12 eV;[6] IE[UO_2^+] = 14.6 ± 0.4 eV;[8] and IE[PuO_2^+] = 15.1 ± 0.4 eV.[8] Equation 8 then gives $\Delta H_f[UO_2^{2+}(g)] = 1533 \pm 39$ kJ mol^{-1}, and $\Delta H_f[PuO_2^{2+}(g)] = 1713 \pm 40$ kJ mol^{-1}. These values agree with those recently reported as follows:[8] $\Delta H_f[UO_2^{2+}(g)] = 1524 \pm 63$ kJ mol^{-1} and $\Delta H_f[PuO_2^{2+}(g)] = 1727 \pm 66$ kJ mol^{-1}.

For Pa, we use $\Delta H_f[PaO_2(g)] = -513 \pm 17$ kJ mol^{-1}[15] and the estimated IEs discussed above: IE[PaO_2] = 5.9 ± 0.5 eV and IE[PaO_2^+] = 16.6 ± 0.4 eV. The resulting enthalpy from eq 8 is $\Delta H_f[PaO_2^{2+}(g)] = 1658 \pm 64$ kJ mol^{-1}.

The intrinsic stability of the bare PaO_2^{2+} ion toward Coulombic dissociation according to eqs 9 and 10 can now be evaluated.

$$PaO_2^{2+} \rightarrow Pa^+ + O_2^+ \quad (9)$$

$$PaO_2^{2+} \rightarrow PaO^+ + O^+ \quad (10)$$

For the process in eq 9 to be endothermic and the dissociation to be thermodynamically unfavorable, the requirement is that $\Delta H_f[PaO_2^{2+}] < \{\Delta H_f[Pa^+] = 1138 \pm 33$ kJ mol^{-1} [40]$\} + \{\Delta H_f[O_2^+] = 1165$ kJ mol^{-1} [30]$\}$: i.e., $\Delta H_f[PaO_2^{2+}] < 2303 \pm 33$ kJ mol^{-1}. For eq 10 to be endothermic and unfavorable, the requirement is that $\Delta H_f[PaO_2^{2+}] < \{\Delta H_f[PaO^+] = 579 \pm 51$ kJ mol^{-1} [52]$\} + \{\Delta H_f[O^+] = 1563$ kJ mol^{-1} [30]$\}$: i.e., $\Delta H_f[PaO_2^{2+}] < 2142 \pm 51$ kJ mol^{-1}. These upper limits indicate that dissociation of PaO_2^{2+} to $\{PaO^+ + O^+\}$ is more energetically favorable than is dissociation to $\{Pa^+ + O_2^+\}$, due to the very strong Pa^+−O bond. Comparison of these upper limits with $\Delta H_f[PaO_2^{2+}(g)] = 1658 \pm 64$ kJ mol^{-1} derived above suggests that bare PaO_2^{2+} is stable toward Coulomb dissociation by at least 300 kJ mol^{-1}. This implies that bare PaO_2^{2+} ion is intrinsically more stable than bare AmO_2^{2+} ion and approximately as stable as bare PuO_2^{2+}.[8]

The ability to prepare AmO_2^{2+}(aq) but not PaO_2^{2+}(aq), and the instability of the Pa(VI) species in general, reflects the inordinate stability of Pa(V) species, notably $PaO(OH)^{2+}$(aq) in aqueous solutions.[20,51] The thermodynamics of the hydrolysis reaction given by eq 11 demonstrates the instability of PaO_2^{2+} in aqueous solution.

$$4PaO_2^{2+}(aq) + 2H_2O(l) \rightarrow 4PaO_2H^{2+}(aq) + O_2(g) \quad (11)$$

The enthalpies of hydration, ΔH_{hyd}, of the three actinyls, UO_2^{2+}, NpO_2^{2+}, and PuO_2^{2+}, are all very similar.[8] If it is assumed that $\Delta H_{hyd}[PaO_2^{2+}] \approx \Delta H_{hyd}[UO_2^{2+}] \approx -1665$ kJ mol^{-1},[8,53] then $\Delta H_f[PaO_2^{2+}(aq)] \approx -885$ kJ mol^{-1} can be derived from $\Delta H_f[PaO_2^{2+}(g)] \approx 1658$ kJ mol^{-1}, according to the procedure described elsewhere.[8,54] Using $\Delta H_f[PaO_2H^{2+}(aq)] = -1113$ kJ mol^{-1},[51] $\Delta H_f[H_2O(l)] = -286$ kJ mol^{-1},[29] and $\Delta H_f[O_2(g)] \equiv 0$, the enthalpy for eq 11 is then estimated as -340 kJ mol^{-1}.

The entropy change for eq 11 can be estimated as 373 J K^{-1} mol^{-1} by employing $S°[PaO_2H^{2+}(aq)] \approx -21$ J mol^{-1} K,[51] $S°[H_2O(l)] = 70$ J K^{-1} mol^{-1},[29] $S°[O_2(g)] = 205$ J K^{-1}mol^{-1},[29] and $S°[PaO_2^{2+}(aq)] \approx S°[UO_2^{2+}(aq)] = -98$ J K^{-1} mol^{-1}.[51] At 298 K, the free energy associated with eq 11 is then ΔG[eq 12] = ΔH[eq 12] − (298 K)ΔS[eq 12] ≈ −451 kJ mol^{-1}. This indicates that eq 11 should be both exothermic, by ca. −340 kJ mol^{-1}, and exoergic, by ca. −451 kJ mol^{-1}. These results are in accord with the nonexistence of an aqueous protactinyl ion, PaO_2^{2+}(aq).

IE of PaO_2^+—Electronic Structure Calculations. Dyall[55] has recently discussed theoretical studies of actinides in unusually high oxidation states, in the form of hypothetical AnO_2F_4 molecules (An = Pu, Cm, Cf, and Fm). In analogy with Dyall's analysis of high-valent, neutral actinide species,[55] one facet of the electronic structure of bare PaO_2^{2+} might relate to the large energy splitting of the $6p_{1/2}$ and $6p_{3/2}$ spinors for the actinides. The four $6p_{3/2}$ spinors are substantially higher in energy than the two $6p_{1/2}$ spinors and, therefore, may be able to participate in the bonding. The result would be chemical engagement of "closed radon core" 6p electrons of Pa.[14] In view of the demonstrated existence and significant stability of PaO_2^{2+} in the gas phase, it is of interest to assess theoretically the electronic structure of it, exploring the possibility of a partial 6p hole.

To obtain an approximate value of the ionization potential of PaO_2^+, we performed a basic-level electronic-structure calculation for this quantity. We used a large-core (78-electron) relativistic effective core potential (RECP) on the Pa-atom[56] and two-electron RECPs on the O-atoms.[57] We used RECP basis sets at approximately the correlation-consistent polarized valence double-ζ (cc-pVDZ) level,[58] (5sd6p4f)/[4sd4p3f] on the Pa-atom, and (4s4p1d)/[2s2p1d] on the O-atoms. In other work,[59] the bond angles were varied for both PaO_2^+ and PaO_2^{2+} and the lowest energies were for the linear structures that are considered here.

A SCF calculation was performed on the (closed shell) $^1\Sigma_g^+$ state of PaO_2^+, assumed to be similar to the ground state of the uranyl ion. Varying the internuclear distance gave a minimum energy value of 1.732 Å. The highest-energy occupied MO was $3\sigma_u$ (Koopmans' theorem ionization potential value of 17.7 eV), followed at modest intervals by $2\pi_u$, $3\sigma_g$, and $1\pi_g$. Thus, an electron was removed from the $3\sigma_u$ MO and a calculation of the $3\sigma_u^1\ ^2\Sigma_u^+$ state of PaO_2^{2+} was carried out. The minimum energy internuclear distance was found to be 1.719 Å. The $3\sigma_u$ MO has principal components of O $2p\sigma$ and Pa $5f\sigma$ character, but all of the MOs change, to some extent, upon ionization. The Mulliken population analyses for these calculations are in Table 3.

TABLE 3: Gross Atomic Populations for PaO_2^+ and PaO_2^{2+}

	PaO_2^+		PaO_2^{2+}	
AO type	Pa	O	Pa	O
s	2.11	3.67	2.09	3.71
p	5.91	8.75	5.75	8.23
d	1.66	0.04	1.64	0.05
f	1.86		1.53	
totals	11.54	12.46	11.01	11.99

Thus, the overall atomic charges for PaO_2^+ are described as approximately $Pa^{+1.46}(O^{-0.23})_2$ and for PaO_2^{2+} as approximately $Pa^{+2.0}(O^{0.0})_2$. The ionized electron comes principally from the

O 2p (0.52), Pa 5f (0.33), and Pa 6p (0.16) atomic orbitals (AOs), as expected from the composition of the $3\sigma_u$ MO. The main effects are the decreased participation of the O 2pσ and Pa 5fσ orbitals in bonding, the increase in positive charge on the Pa-atom, and the decreased magnitude of effective negative charge on the O-atoms. A smaller effect is the enlargement of the hole in the 6p shell on the Pa-atom (0.09−0.25 electrons). A description of the ionization in terms of oxidation numbers would need to include a reduction in the magnitude of the oxygen oxidation number. The (adiabatic) ionization potential was calculated to be 16.56 eV. With only a modest change in internuclear distance, the vertical ionization potential would be only slightly higher. No corrections for zero-point energy were made.

These calculations were later improved by adding a set of g orbitals on the Pa atom and adding electron correlation with single- and double-excitation configuration interaction (CI). There were surprisingly small changes in the results. The charge distribution was little changed. The bond distance of PaO_2^{2+} became 1.730 Å. The ionization potential became 16.61 eV.

Conclusions

The Pa^+ ion was efficiently oxidized by each of the seven oxidants studied (see Table 1), indicating a strong metal−oxygen bond—specifically, $D[Pa^+-O] \geq 751$ kJ mol^{-1}; it is estimated that $D[Pa^+-O] = 800 \pm 50$ kJ mol^{-1}. On the basis of the oxidation behavior of PaO^+, it was also shown that $D[OPa^+-O] \geq 751$ kJ mol^{-1}, suggesting that the second bond in PaO_2^+ is nearly as strong as that in PaO^+.

The Pa^{2+} ion was oxidized by CH_2O, indicating that $D[Pa^{2+}-O] \geq 751$ kJ mol^{-1}. Surprisingly, the dipositive protactinium monoxide was efficiently oxidized to PaO_2^{2+} by N_2O. The PaO_2^{2+} moiety is not found in condensed-phase chemistry, as Pa(V) is the highest accessible oxidation state there. In view of the importance of uranyl and heavier actinyls, AnO_2^{2+} (An = U, Np, Pu, and Am), in condensed-phase chemistry, bare PaO_2^{2+} is considered intriguing in the context of actinide science. The actinyl connectivity, $\{O-Pa-O\}^{2+}$, was indicated by CID experiments. The IE of PaO_2^+ was estimated as 16.6 ± 0.4 eV based on the rate constant for electron transfer from CO to PaO_2^{2+}. It is possible to evaluate the stability of PaO_2^{2+} toward Coulomb explosion—$\{PaO^+ + O^+\}$ is the energetically favored dissociation channel but is endothermic by ~300 kJ mol^{-1}.

To illuminate the nature of PaO_2^{2+}, SCF and CI calculations were performed on PaO_2^+ and PaO_2^{2+}. The calculated IE-$[PaO_2^+] = 16.61$ eV is in remarkably good agreement with the experimental value, providing confidence in the validity of both approaches. The SCF and CI results indicate the electron removed from the very stable pentavalent PaO_2^+ species to produce PaO_2^{2+} comes from O 2p (0.52), Pa 5f (0.33), and Pa 6p (0.16). This indicates that the ionized electron comes primarily from a bonding MO of the PaO_2^{2+} ion with a smaller amount from the Pa 6p shell.

PaO_2^{2+} was found to catalyze the oxidation of CO by N_2O. PaO^{2+} is oxidized to PaO_2^{2+} by N_2O; the PaO_2^{2+} then oxidizes CO to CO_2, thereby regenerating PaO^{2+}. Several examples of this type of process are known for monopositive metal oxides; to the best of our knowledge, this is the first known example of such O-atom transport via a dipositive metal oxide ion. The overall catalytic cycle is rather inefficient for PaO_2^{2+} due to electron transfer from N_2O and CO to produce the inert monopositive dioxide, PaO_2^+. The PaO_2^{2+} ion was also found to react with H_2, forming PaO_2H^{2+}, which is a stable Pa(V) ion that can be produced in aqueous solution.

Thus, FTICR-MS studies of reactions of bare and ligated, monopositive, and dipositive ions have revealed new chemistry for Pa. Several of the observed reactions with Pa ions, and their kinetics, are in accord with known and predictable thermodynamics and electronic properties. However, the formation of the novel, formally hexavalent oxide ion, PaO_2^{2+}, was an unexpected finding. This species, corresponding to protactinyl, is particularly significant in view of the important role of other actinyls in condensed-phase chemistry. Theoretical calculations indicate that electronic charge is lost from both the Pa- and the O-atoms in forming PaO_2^{2+} from PaO_2^+.

Acknowledgment. This work was supported by Fundação para a Ciência e a Tecnologia (FCT) and by POCI 2010 (cofinanced by FEDER), under Contracts POCTI/35364/QUI/2000 and POCI/QUI/58222/2004; by the U.S. Department of Energy, Office of Basic Energy Sciences (U.S. DOE/OBES), Grant ER15136; and by the U.S. DOE/OBES under Contract DE-AC05-00OR22725 with Oak Ridge National Laboratory, managed and operated by UT-Battelle, LLC. M.S. is grateful to FCT for a Ph.D. grant.

References and Notes

(1) (a) Armentrout, P. B.; Beauchamp, J. L. *Acc. Chem. Res.* **1989**, 22, 315−321. (b) Eller, K.; Schwarz, H. *Chem. Rev.* **1991**, *91*, 1121−1177. (c) Freiser, B. S. *J. Mass Spectrom.* **1996**, *31*, 703−715. (d) Schröder, D.; Schwarz, H. *J. Phys. Chem. A* **1999**, *103*, 7385−7394. (e) Schwarz, H. *Angew. Chem., Int. Ed.* **2003**, *42*, 4442−4454. (f) Schwarz, H. *Int. J. Mass Spectrom.* **2004**, *237*, 75−105.

(2) Schröder, D.; Schwarz, H.; Clemmer, D. E.; Chen, Y.; Armentrout, P. B.; Baranov, V. I.; Böhme, D. K. *Int. J. Mass Spectrom. Ion Processes* **1997**, *161*, 175−191.

(3) Some representative examples: (a) Schilling, J. B.; Beauchamp, J. L. *J. Am. Chem. Soc.* **1988**, *110*, 15−24. (b) Sunderlin, L. S.; Armentrout, P. B. *J. Am. Chem. Soc.* **1989**, *111*, 3845−3855. (c) Yin, W. W.; Marshall, A. G.; Marçalo, J.; Pires de Matos, A. *J. Am. Chem. Soc.* **1994**, *116*, 8666−8672. (d) Cornehl, H. H.; Heinemann, C.; Schröder, D.; Schwarz, H. *Organometallics* **1995**, *14*, 992−999. (e) Cornehl, H. H.; Hornung, G.; Schwarz, H. *J. Am. Chem. Soc.* **1996**, *118*, 9960−9965. (f) Marçalo, J.; Pires de Matos, A.; Evans, W. J. *Organometallics* **1997**, *16*, 3845−3850. (g) Carretas, J. M.; Pires de Matos, A.; Marçalo, J.; Pissavini, M.; Decouzon, M.; Géribaldi, S. *J. Am. Soc. Mass Spectrom.* **1998**, *9*, 1035−1042. (h) Koyanagi, G. K.; Böhme, D. K. *J. Phys. Chem. A* **2001**, *105*, 8964−8968. (i) Marçalo, J.; Pires de Matos, A. *J. Organomet. Chem.* **2002**, *647*, 216−224. (j) Carretas, J. M.; Marçalo, J.; Pires de Matos, A. *Int. J. Mass Spectrom.* **2004**, *234*, 51−61. (k) Koyanagi, G. K.; Zhao, X.; Blagojevic, V.; Jarvis, M. J. Y.; Böhme, D. K. *Int. J. Mass Spectrom.* **2005**, *241*, 189−196.

(4) Some representative examples: (a) Johnsen, R.; Biondi, M. A. *J. Chem. Phys.* **1972**, *57*, 1975−1979. (b) Armentrout, P. B.; Hodges, R. V.; Beauchamp, J. L. *J. Chem. Phys.* **1977**, *66*, 4683−4688. (c) Armentrout, P. B.; Beauchamp, J. L. *Chem. Phys.* **1980**, *50*, 27−36. (d) Armentrout, P. B.; Beauchamp, J. L. *J. Phys. Chem.* **1981**, *85*, 4103−4105. (e) Heinemann, C.; Cornehl, H. H.; Schwarz, H. *J. Organomet. Chem.* **1995**, *501*, 201−209. (f) Marçalo, J.; Leal, J. P.; Pires de Matos, A. *Int. J. Mass Spectrom. Ion Processes* **1996**, *157/158*, 265−274. (g) Marçalo, J.; Leal, J. P.; Pires de Matos, A. *Organometallics* **1997**, *16*, 4581−4588. (h) Schröder, D.; Diefenbach, M.; Klapötke, T. M.; Schwarz, H. *Angew. Chem., Int. Ed.* **1999**, *38*, 137−140. (i) Vieira, M. C.; Marçalo, J.; Pires de Matos, A. *J. Organomet. Chem.* **2001**, *632*, 126−132. (j) Moulin, C. *Radiochim. Acta* **2003**, *91*, 651−657 and references therein. (k) Gresham, G. L.; Gianotto, A. K.; Harrington, P. B.; Cao, L.; Scott, J. R.; Olson, J. E.; Appelhans, A. D.; Van Stipdonk, M. J.; Groenewold, G. S. *J. Phys. Chem. A* **2003**, *107*, 8530−8538. (l) Van Stipdonk, M. J.; Chien, W.; Anbalagen, V.; Bulleigh, K.; Hanna, D.; Groenwold, G. S. *J. Phys. Chem. A* **2004**, *108*, 10448−10457. (m) Chien, W.; Anbalagan, V.; Zandler, M.; Van Stipdonk, M. J.; Hanna, D.; Gresham, G.; Groenewold, G. *J. Am. Soc. Mass Spectrom.* **2004**, *15*, 777−783. (n) Groenewold, G. S.; Van Stipdonk, M. J.; Gresham, G. L.; Chien, W.; Bulleigh, K.; Howard, A. *J. Mass Spectrom.* **2004**, *39*, 752−761.

(5) (a) Gibson, J. K. *J. Am. Chem. Soc.* **1998**, *120*, 2633−2640. (b) Gibson, J. K. *Int. J. Mass Spectrom.* **2002**, *214*, 1−21 and references therein. (c) Gibson, J. K.; Marçalo, J. *Coord. Chem. Rev.* **2006**, in press (available online 4 Nov 2005), and references therein.

(6) Santos, M.; Marçalo, J.; Pires de Matos, A.; Gibson, J. K.; Haire, R. G. *J. Phys. Chem. A* **2002**, *106*, 7190−7194.

(7) Santos, M.; Marçalo, J.; Leal, J. P.; Pires de Matos, A.; Gibson, J. K.; Haire, R. G. *Int. J. Mass Spectrom*. **2003**, *228*, 457−465.

(8) Gibson, J. K.; Haire, R. G.; Santos, M.; Marçalo, J.; Pires de Matos, A. *J. Phys. Chem. A* **2005**, *109*, 2768−2781.

(9) Gibson, J. K.; Haire, R. G. *Inorg. Chem.* **2002**, *41*, 5897−5906.

(10) (a) Smith, J. L.; Kmetko, E. A. *Less-Common Met. 90*, **1983**, 83−88. (b) Haire, R. G.; Heathman, S.; Idiri, M.; Le Bihan, T.; Lindbaum, A.; Rebizant, J. *Phys. Rev. B* **2003**, *67*, 134101-1−134101-10.

(11) Brooks, M. S. S.; Calestani, G.; Spirlet, J. C.; Rebizant, J.; Müller, W.; Fournier, J. M.; Blaise, A. *Physica B* **1980**, *102*, 84−87.

(12) (a) Kaltsoyannis, N.; Bursten, B. E. *Inorg. Chem*. **1995**, *34*, 2735−2744. (b) Straka, M.; Hrobárik, P.; Kaupp, M. *J. Am. Chem. Soc*. **2005**, *127*, 2591−2599.

(13) Dyall, K. G. *Mol. Phys.* **1999**, *96*, 511−518.

(14) Straka, M.; Dyall, K. G.; Pyykkö, P. *Theor. Chem. Acc*. **2001**, *106*, 393−403.

(15) Kleinschmidt, P. D.; Ward, J. W. *J. Less-Common Met*. **1986**, *121*, 61−66.

(16) Gagliardi, L.; Roos, B.; Malmqvist, P.-A.; Dyke, J. M. *J. Phys. Chem. A* **2001**, *105*, 10602−10606.

(17) Heinemann, C.; Cornehl, H. H.; Schröder, D.; Dolg, M.; Schwarz, H. *Inorg. Chem.* **1996**, *35*, 2463−2475.

(18) Brönstrup, M.; Schröder, D.; Kretzschmar, I.; Schwarz, H.; Harvey, J. N. *J. Am. Chem. Soc*. **2001**, *123*, 142−147.

(19) Cornehl, H. H.; Wesendrup, R.; Diefenbach, M.; Schwarz, H. *Chem. Eur. J.* **1997**, *3*, 1083−1090.

(20) Kirby, H. W. In *The Chemistry of the Actinide Elements*, 2nd ed.; Katz, J. J., Seaborg, G. T., Morss, L. R., Eds.; Chapman and Hall: London, 1986; Chapter 4 (Protactinium), pp 102−168.

(21) Marçalo, J.; Pires de Matos, A.; Evans, W. J. *Organometallics* **1996**, *15*, 345−349.

(22) Perrin, D. D.; Armarego, W. L. F. *Purification of Laboratory Chemicals*, 3rd ed.; Pergamon Press: Oxford, 1988.

(23) Bruce, J. E.; Eyler, J. R. *J. Am. Soc. Mass Spectrom.* **1992**, *3*, 727−733.

(24) Lin, Y.; Ridge, D. P.; Munson, B. *Org. Mass Spectrom.* **1991**, *26*, 550−558.

(25) Bartmess, J. E.; Georgiadis, R. M. *Vacuum* **1983**, *33*, 149−153.

(26) Lide, D. R., Ed. *CRC Handbook of Chemistry and Physics*, 75th ed.; CRC Press: Boca Raton, 1994.

(27) Guan, S.; Marshall, A. G. *Int. J. Mass Spectrom. Ion Processes* **1996**, *157/158*, 5−37.

(28) Su, T.; Chesnavich, W. J. *J. Chem. Phys.* **1982**, *76*, 5183−5185.

(29) NIST Chemistry Webbook−NIST Standard Reference Database Number 69, June 2005 Release (http://webbook.nist.gov/chemistry/).

(30) Lias, S. G.; Bartmess, J. E.; Liebman, J. F.; Holmes, J. L.; Levin, R. D.; Mallard, W. G. *J. Phys. Chem. Ref. Data* **1988**, *17* (Suppl. 1).

(31) Jackson, G. P.; King, F. L.; Goeringer, D. E.; Duckworth, D. C. *J. Phys. Chem. A* **2002**, *106*, 7788−7794.

(32) Liang, B.; Hunt, R. D.; Kushto, G. P.; Andrews, L.; Li, J.; Bursten, B. E. *Inorg. Chem.* **2005**, *44*, 2159−2168.

(33) Blaise, J.; Wyart, J.-F. *International Tables of Selected Constants 20−Energy Levels and Atomic Spectra of Actinides*; Tables Internationales de Constantes: Paris, 1992; available on the web at http://www.lac.u-psud.fr/Database/Contents.html.

(34) Goncharov, V.; Han, J.; Kaledin, L. A.; Heaven, M. C. *J. Chem. Phys.* **2005**, *122*, 204311-1−204311-6.

(35) (a) Han, J. D.; Kaledin, L. A.; Goncharov, V.; Komissarov, A. V.; Heaven, M. C *J. Am. Chem. Soc.* **2003**, *125*, 7176−7177. (b) Han, J. D.; Goncharov, V.; Kaledin, L. A.; Komissarov, A. V.; Heaven, M. C. *J. Chem. Phys.* **2004**, *120*, 5155−5163.

(36) Gibson, J. K.; Haire, R. G.; Marçalo, J.; Santos, M.; Pires de Matos, A.; Leal, J. P. *J. Nucl. Mater*. **2005**, *344*, 24−29.

(37) Sugar, J. *J. Chem. Phys.* **1973**, *59*, 788−791.

(38) Gibson, J. K. *J. Phys. Chem. A* **2003**, *107*, 7891−7899.

(39) Hildenbrand, D. L.; Gurvich, L. V.; Yungman, V. S. *The Chemical Thermodynamics of Actinide Elements and Compounds*; IAEA: Vienna, 1985; Part 13−The Gaseous Actinide Ions.

(40) Heinemann, C.; Schwarz, H. *Chem. Eur. J.* **1995**, *1*, 7−11.

(41) Cornehl, H. H.; Heinemann, C.; Marçalo, J.; Pires de Matos, A.; Schwarz, H. *Angew. Chem., Int. Ed. Engl*. **1996**, *35*, 891−894.

(42) Lavrov, V. V.; Blagojevic, V.; Koyanagi, G. K.; Orlova, G.; Bohme, D. K. *J. Phys. Chem. A* **2004**, *108*, 5610−5624.

(43) Zhou, M.; Andrews, L. *J. Chem. Phys.* **1999**, *111*, 11044−11049.

(44) Katz, J. J.; Morss, L. R.; Seaborg, G. T. In *The Chemistry of the Actinide Elements*, 2nd ed.; Katz, J. J., Seaborg, G. T., Morss, L. R., Eds.; Chapman and Hall: London, 1986; Chapter 14 (Summary and Comparative Aspects of the Actinide Elements), pp 1121−1195.

(45) Roth, L. M.; Freiser, B. S. *Mass Spectrom. Rev.* **1991**, *10*, 303−328.

(46) Spears, K. G.; Fehsenfeld, G. C.; McFarland, M.; Ferguson, E. F. *J. Chem. Phys.* **1972**, *56*, 2562−2566.

(47) The "actinyl" terminology here refers to the doubly charged AnO_2^{2+} species, not monopositive dioxo ions such as PaO_2^+ and NpO_2^+.

(48) Kappes, M. M.; Staley, R. H. *J. Am. Chem. Soc.* **1981**, *103*, 1286−1287.

(49) (a) Blagojevic, V.; Orlova, G.; Bohme, D. K. *J. Am. Chem. Soc.* **2005**, *127*, 3545−3555. (b) Bohme, D. K.; Schwarz, H. *Angew. Chem., Int. Ed.* **2005**, *44*, 2336−2354 and references therein.

(50) It should be noted that the distinctive and large fullerene ions such as C_{60}^{2+} have been shown to exhibit somewhat different electron-transfer behavior−See, for example, Petrie, S.; Javahery, G.; Wang, J.; Bohme, D. K. *J. Phys. Chem*. **1992**, *96*, 6121−6123.

(51) Morss, L. R. In *The Chemistry of the Actinide Elements*, 2nd ed.; Katz, J. J., Seaborg, G. T., Morss, L. R., Eds.; Chapman and Hall: London, 1986; Chapter 17 (Thermodynamic Properties), pp 1278−1360.

(52) Derived in a previous section.

(53) Moskaleva, L. V.; Krüger, S.; Spörl, A.; Rösch, N. *Inorg. Chem.* **2004**, *43*, 4080−4090.

(54) Rizkalla, E. N.; Choppin, G. R. In *Handbook on the Physics and Chemistry of Rare Earths*; Gschneidner, K. A., Jr., Eyring, L., Choppin, G. R., Lander, G., Eds.; North-Holland: Amsterdam, 1994; Vol. 18: Lanthanides/Actinides, pp 529−558.

(55) Dyall, K. G. *Chem. Phys.* **2005**, *311*, 19−24.

(56) Ermler, W. C.; Ross, R. B.; Christiansen, P. A. *Int. J. Quantum Chem.* **1991**, *40*, 829−846.

(57) Pacios, L. F.; Christiansen, P. A. *J. Chem. Phys.* **1985**, *82*, 2664−2671.

(58) Blaudeau, J.-P.; Brozell, S. R.; Matsika, S.; Zhang, Z.; Pitzer, R. M. *Int. J. Quantum Chem.* **2000**, *77*, 516−520.

(59) Yang, T. Private communication.